Eurasian Chem.-Technol. J. 27 (2025) 89–100
The journal of the Institute of Combustion Problems https://ect-journal.kz

https://doi.org/10.18321/ectj1657

Features of the Structure and Properties of the ta-C Coatings Deposited from Filtered Flows of the Pulsed Cathodic-Arc Discharge

Yang Gao[1], K.A. Sakhovsky[2], Shangzhe Jiang[1,3], S.Y. Chepkasov[4], Xiaohong Jiang[1]*, A.S. Rudenkov[1,2], Urol K. Makhmanov[5], D.G. Piliptsou[1,2], A.V. Rogachev[1,2]**

[1]International Chinese-Belorussian Scientific Laboratory on Vacuum Plasma Technology, Nanjing University of Science and Technology, 200 Xiaolingwei str., Nanjing, 210094, China
[2]Francisk Skorina Gomel State University, 104 Sovetskaya str., Gomel, 246019, Belarus
[3]British School of Nanjing, 16 Hanfu str., Nanjing, 211116, China
[4]Physical Department, 4 Novosibirsk State University, Pirogova str., 630090, Novosibirsk, Russia
[5]Institute of Ion-Plasma and Laser Technologies, Uzbekistan Academy of Sciences, Tashkent 100125, Uzbekistan

Article info

Received:
4 February 2025

Received in revised form:
29 March 2025

Accepted:
5 May 2025

Keywords:
Carbon coating
Morphology
Phase
Roughness
Nanohardness
Clusters

Abstract

The amorphous carbon (ta-C) coatings have been deposited on the polished silicon (111) substrates using the pulsed cathodic-arc evaporation of the graphite target. A comparative analysis of the structure and properties of the ta-C coatings deposited via the pulsed cathodic-arc evaporation with different pulse voltages has been carried out. According to the Raman analyses, optimal energy modes and arc voltage for generating pulsed flows of carbon plasma have been determined. Using the electromagnetic filter enables the effective separation of the ionic and droplet components of the coating while ensuring the complete removal of the macroparticles from the plasma flow. The surface of the coatings deposited under different separation modes, as well as different discharge voltages, has been studied via scanning electron and atomic force microscopies. This leads to a twofold decrease in the surface roughness compared to the flow without filtration. In addition, an increase in the hardness and elasticity modulus of the coatings has been detected. The optical parameters of the coatings depend directly on the phase composition of the coatings, which is controlled by the sp^2/sp^3 ratio, and on the parameters of the microstructure (size, number and ordering of sp^2 clusters). The application of filters enables the deposition of coatings composed of amorphous carbon that exhibit high mechanical and optical properties. These coatings are notably thinner when compared to those deposited from flows without filtration. This study determines the structure, mechanical, and optical properties of a-C coatings deposited with and without filtration of pulsed plasma carbon flow, maintaining a constant discharge duration.

1. Introduction

The development of carbon coatings deposition methods and active research on their structure and properties began in the early 1970s [1, 2]. The ongoing advancement of vacuum technology and diverse evaporator designs has led to an impressive rise in publications concerning methods for carbon coating formation, as well as their structural characteristics and properties. This growth has subsequently broadened the applications of carbon-based coatings in fields such as medicine, optics, and corrosion protection.

The properties of carbon coatings are influenced not just by carbon atoms with sp^1, sp^2 and sp^3 bond hybridization, but also by the size and degree of ordering of clusters created by carbon atoms with other bond hybridization types [3]. Structural defects such as surface deterioration, pore formation or the presence of droplets on the surface caused by specific evaporator working characteristics significantly reduce the structural quality and, therefore, the exploitation properties of the coated surface.

*Corresponding author.
E-mail address: jiangxh24@njust.edu.cn

Carbon-based coatings can be divided into two large groups: hydrogen-containing (a-C:H) and hydrogen-free (a-C) coatings, which have significantly different properties due to the presence of both hydrogen and C-H compounds in the coating volume.

Tetrahedral carbon (ta-C) coatings stand out among the variety of hydrogen-free a-C coatings due to their higher hardness, wear resistance, refractive index, and low friction coefficient compared to a-C:H coatings [1, 2]. The mechanical properties of ta-C coatings are commensurate with diamond [4, 5] due to the similarity of their structures.

Usually, ta-C coatings are fabricated by physical sputtering (PVD) methods, particularly pulsed cathodic-arc (PCA) sputtering. The distinctive features of PCA sputtering include a low deposition temperature, which enables the use of substrates with low thermal resistance, and the high energy of carbon ions in the flux, facilitating the preferential growth of Csp^3 clusters. This allows for the deposition of ta-C coatings that demonstrate high stability in both mechanical and optical properties [6].

Another characteristic of PCA methods is the evaporation of the graphite cathode from the cathode spots that are formed by intense pulsed discharge. Short discharge duration combined with a high pulse power leads to an explosive ejection of material from the cathode surface, partial ionization and the generation of macroparticles as products of cathode erosion [7, 8].

A very dense carbon plasma is generated near the cathode surface, resulting in numerous collisions between electrons and ions/atoms/macroparticles of carbon. This interaction leads to a partial degradation of macroparticles and a reduction in the ionic component energy. With the further expansion of the plasma into the vacuum, the number of collisions is significantly reduced, decreasing the ionization degree and the appearance of neutral graphite macroparticles in the flux [9]. Graphite macroparticles range from hundreds of nanometers to several micrometers in size depending on spatiotemporal and energy regimes of evaporation [10, 11].

When reaching the substrate, macroparticles attach to its surface, form volumetric defects, act as stress concentrators, and significantly change the surface topography and roughness, leading to the reduced wear resistance of the coating and its delamination during friction. The presence of soft macroparticles in the coating under friction conditions leads to the initiation of coating failure by their chipping and increased abrasive wear. In addition, the presence of graphite-structured macroparticles also deteriorates the optical properties of the coating and initiates penetrating corrosion in chemically aggressive environments [12, 13].

Various techniques can be applied to regulate the macroparticles to ion component ratio in the pulsed carbon plasma flux. These include modifying the energy and duration of the discharge pulse [14-16], implementing inclined deposition from the normal to the substrate [10], and employing magnetic stabilization of the cathode spot along with magnetic focusing of the plasma flux [17]. These methods enhance the control of cathode spot movement on the cathode surface and enable the separation of macroparticles from the ionic component of the flux by directing it to the substrate surface.

However, previous studies [18-20] indicate that the most effective removal of macroparticles from the plasma flux is accomplished through the application of electromagnetic filters that generate external fields. These fields influence the trajectories of both charged (ionic) and neutral (macroparticle) components within the flux. There is a variety of such filters, distinguished by their construction (geometry, presence of additional screens) and method of arrangement (in-chamber, free-standing or located outside the vacuum chamber in the case), which are described in detail in many reviews [1, 21]. Noteworthy is that most of the studies focus on the coating deposition from stationary carbon plasma flows (filtered cathodic vacuum arc (FCVA)), as well as on the development and optimization of filters for such evaporators. Thus, the separation of stationary carbon plasma flows is carried out by filters, in which magnetic fields are created by external electromagnets. Therefore, the design of commercially available evaporators includes a filter, power supplies for the magnetic system, and a magnetic field and discharge synchronization system, which leads to a substantial increase in both the cost and the dimensions of the equipment, while significantly less attention is paid to the devices for pulsed flows filtration.

Sources of pulsed plasma flows have all the above-mentioned problems inherent to stationary evaporators. Moreover, a filter, being a solenoid included in the construction of the pulse evaporator, possesses high inductance, resulting in a change of duration and amplitude values of the current pulse as the discharge pulse current passes through it. This affects the process of plasma flow generation and ion energy in the flow, leading to an increased thermal load on the substrate, which in turn causes structural and phase composition changes in the coatings.

In this work, the structure, mechanical and optical properties of a-C coatings deposited with/without filtration of pulsed plasma carbon flux at a constant discharge duration have been determined.

2. Experimental

The ta-C coatings were deposited on the polished silicon (111) substrates using the pulsed vacuum arc method. The experimental setups with and without plasma filtration are schematically illustrated in Fig. 1.

The graphite cathode (MPG-6, purity 99.9%) evaporated during a pulsed high-current arc discharge in the carbon plasma source. Auxiliary ignition discharges in the ignition power unit (Fig. 1) ensured stable excitation of the main pulsed discharge by energy stored in the capacitor battery of the power unit, the electrical capacity of which is 2150 μF (Fig. 1, a).

Deposition of coatings was conducted under the following discharge parameters: pulse duration from 275 μs, pulse frequency set at 5 Hz, amplitude value of the discharge current ranging from 1.5 to 5.5 kA (variable with voltage), and initial discharge voltage between 200 and 450 V.

A feature of the carbon plasma generated by pulsed cathodic-arc discharge is a wide ion energy range (20–100 eV), which can be regulated by changing the discharge voltage.

Research indicates [22] that in pulsed cathodic-arc plasma sources, the discharge current can reach several kiloamperes, enabling the generation of a magnetic field for plasma transport. Therefore, a free-standing quarter-torus filter with an inner diameter of 95 mm and a length of 380 mm, bent at 90°, is positioned inside the vacuum chamber and connected in series to the main discharge circuit. The current pulse passing through the solenoid generates a magnetic field sufficient to alter the trajectory of the ion flow (Fig. 1b). The operational principle of the curved filter is based on magnetized electrons spiraling along the curved magnetic field lines. Through Coulomb interaction, these electrons drag along the relatively heavy ions, for which the Larmor radius significantly exceeds the filter's radius. Neutral particles are not deflected by the magnetic field and exit the plasma transport channel. Since the transport of carbon plasma from the cathode surface to the substrate occurred in the curved magnetic field of a toroidal solenoid (which possesses inductance), this modified the parameters of the discharge L-C circuit. As a result, the pulse duration increased, leading to a reduction in the electron flux density at the surface of the graphite cathode.

Therefore, to ensure an accurate comparison of coating deposition results obtained with and without plasma flow filtration, the filter was incorporated into the anode circuit outside the vacuum chamber. This configuration functioned as an inductance L (Fig. 1a), which increased the discharge duration.

In order to investigate how coating structure depends on evaporation conditions, specifically discharge voltage (which governs particle density and energy in the plasma flow and affects macroparticle formation leading to surface morphology changes), coatings were deposited at discharge voltages varying from 200 to 450 V without a filter (Fig. 1, a). The discharge pulse repetition rate was maintained at 5 Hz with a total of 1000 pulses.

The chemical composition of the coatings was analyzed by X-ray photoelectron spectroscopy (XPS) using a PHI Quantera II spectrometer (ULVAC-PSI, Inc., Japan). The spectra were calibrated using the C1s line with a binding energy of 284.6 eV.

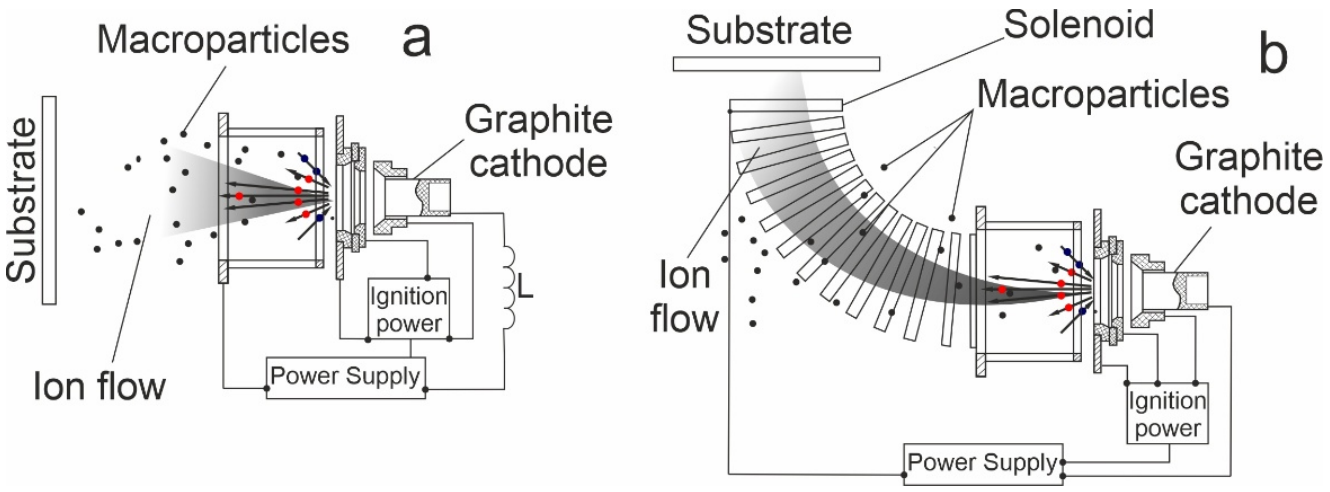

Fig. 1. Schematic of the ta-C coatings deposition: a – without plasma filtration, b – with plasma filtration.

The spectra postprocessing was carried out in XPS PEAK software. The ratio of carbon bonds with sp^3- and sp^2-hybridizations was determined by the relative contribution of the corresponding peak to the area limited by the bonding energy axis and the contour of the C1s peak. The background spectrum was simulated using the Shirley function.

The structure of the coatings was studied by Raman spectroscopy using the Horiba T64000 spectrometer (Horiba-Jobin Yvon, Japan). The spectra were excited by laser radiation with a wavelength of 514.5 nm and a power of 3 mW. The spectra were recorded in the range of 1050–1900 cm^{-1}.

The surface of the samples was examined by scanning electron microscopy (SEM) using the JEOL JSM-6700F instrument (JEOL, Japan). The SEM images were obtained at an accelerating voltage of 15 kV and a working distance of 6 mm. SEM samples were pre-coated with a thin layer of gold to reduce the charging induced by the electron beam.

The surface morphology and phase distribution were studied by a Solver-Pro P47 (NT-MDT, Russia) atomic force microscope (AFM). The surface roughness parameters were determined after the mathematical processing of the three-dimensional topography image.

Hardness and elastic modulus were determined via the nanoindentation method in the mode with the linear sweep of applied loading force using the NanoScan-4D nanohardness tester (FSBI TISNCM, Russia). Indentation was carried out according to the standard method (ISO 14577) [23, 24] with a single loading and unloading. According to ISO 14577, the indenter is pressed into the surface with a given law of increasing force or penetration depth. After reaching the maximum load or penetration depth, the indenter remains motionless for a specified duration before being withdrawn from the sample surface. For accurate measurements, it is essential to maintain the ambient temperature within the range of 23±5 °C, while ensuring that the relative humidity does not surpass 50%. To prevent the substrate from affecting the measurements of hardness and Young's modulus in thin films, the indenter's penetration depth must not surpass 10–20% of the film thickness. To ensure statistically reliable data, 15 measurements were carried out on each coating sample under identical loading conditions, and then the results were averaged. The maximum load on the Berkovich diamond indenter was 5 mN.

The optical transmittance and absorbance measurements were performed in the range of 200–1100 nm using a UV-visible spectrophotometer Cary-50 (Varian). The optical band gap E_g of the coatings was calculated via the Tauc formula [25].

The thickness (d), refractive index (n) and extinction coefficient (k) of the coatings were measured through ellipsometry with the LEF-752 (ISP SB RAS, Russia) instrument, which operated at a wavelength of 632 nm in multiple-angle-of-incidence measurement mode. The incidence angle for the light beam was varied between 45 and 70° with a step of 5°. The “uniform coating-substrate” model was chosen to evaluate d, n, and k using the established optical constants of the substrate.

3. Results and Discussion

The initial discharge voltage is a critical parameter for the deposition of ta-C coatings using pulsed vacuum cathodic arc discharge. This voltage determines the carbon ion flux density and energy, which subsequently affects substrate temperature and leads to the formation of a carbon matrix with various sp^2/sp^3 ratios. In the discharge voltage range of 250–400 V, stable discharge pulses are achieved, with carbon ion energies of 50–80 eV, which represents sufficient and necessary conditions for preferential formation of C-Csp^3 bonds [26]. When depositing ta-C coatings using pulsed arc discharge, the structure shows a complex dependence on deposition energy:

1. As carbon ion energy (discharge voltage) entering the substrate increases, the temperature of the substrate rises due to surface bombardment and the annealing process of the developing coating, thereby promoting the growth of a more energetically favorable graphitic component [26].

2. Higher discharge voltages increase carbon ion energy, enhancing subplantation depth of carbon atoms. According to Lifshitz theory [27], this activates defect generation that reduces the probability of $sp^3 \rightarrow sp^2$ transformation in the carbon matrix.

3. At high pulse currents, significant cathode material erosion occurs, introducing numerous macroparticles into the plasma that increase coating roughness and graphitization.

Consequently, the formation of a coating structure with varying sp^2/sp^3 hybridization ratios is influenced by the subplantation growth mechanism, the annealing of the developing coating by incoming carbon ions, and the adherence of macroparticles originating from cathode fragments to the substrate.

To determine the optimal discharge voltage for producing ta-C with high sp^3 bond content, the coatings were deposited at various voltages without flow filtration, followed by structural characterization using Raman spectroscopy (Fig. 2).

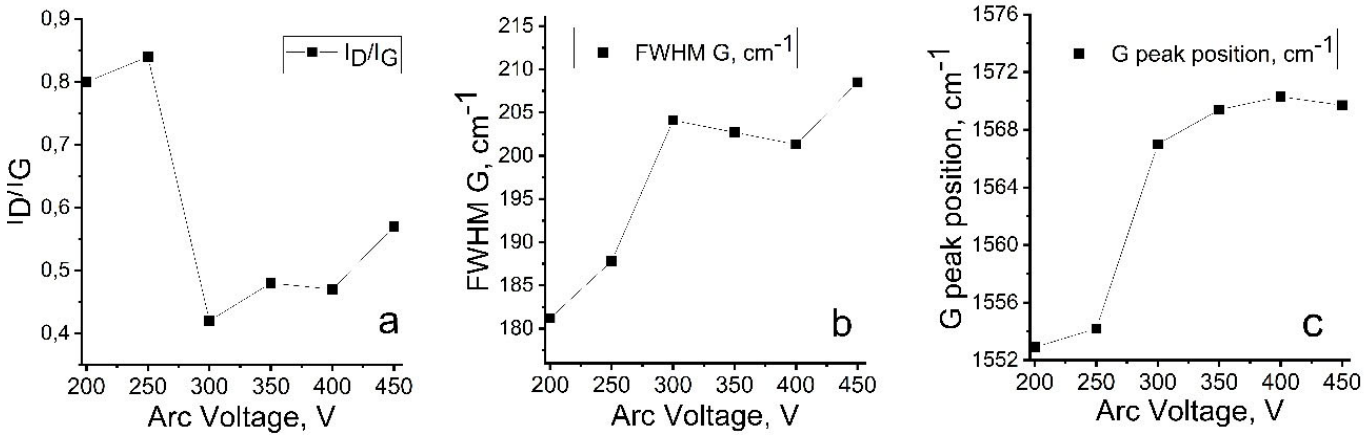

Fig. 2. Parameters of Raman spectra for ta-C coatings deposited at different discharge voltages without flow filtration.

Although Raman spectroscopy does not provide definitive insights into the structure of carbon-based coatings, it continues to be a prevalent technique for structural analysis, evaluating structural ordering and comparing the relative content of sp^2 and sp^3 carbon atoms. As established in [28], graphite exhibits higher structural ordering in comparison to amorphous diamond-like coatings. Therefore, an increase in the concentration of sp^3 bonds within the coating structure leads to a noticeable decrease in its overall ordering.

The structural parameters of ta-C coatings are reflected in the shift of the G-peak position, its full width at half maximum (FWHM), and the I_D/I_G intensity ratio. These parameters indicate changes in the degree of structural ordering in carbon coatings.

An increase in the I_D/I_G ratio suggests a higher concentration of ordered aromatic rings within clusters and a reduction of single bonds in linear C–C chains [29]. Figure 2, a illustrates that at low discharge voltages (up to 250 V), the I_D/I_G ratio reaches its maximum values, signifying a substantial presence of aromatic rings. When the voltage increases to 300 V, the I_D/I_G ratio sharply decreases to its minimum. Further voltage elevations (beyond 300 V) lead to a slight rise in the I_D/I_G ratio, suggesting a minor increase in aromatic ring formation within the coating structure.

As stated in [30], the shift of the G peak in ta-C coatings towards higher frequencies may indicate an increase in the sp^3 content and is due to a change in the sp^2 configuration from rings to olefinic groups. Olefinic C=C bonds have a higher frequency because they are shorter than aromatic bonds. Findings demonstrate that increasing discharge voltage induces a shift of the G-peak towards higher frequencies. Notably, at a discharge voltage of 400 V, the G-peak position reaches its maximum value, suggesting an increased disorder and, consequently, enhanced sp^3 phase formation in the coating. At discharge voltages below 300 V, a graphite-like structure predominates [31].

The FWHM of the G-peak serves as a primary parameter characterizing structural disorder, determined by bond angle distortions between carbon atoms. The observed dependence of FWHM (G) on discharge voltage (Fig. 2, b) reveals that at a discharge voltage of 300 V, a notable level of disordered structure is present, which subsequently diminishes as the discharge voltage increases.

Hence, as evidenced by Fig. 2, a discharge voltage of 300 V can be considered optimal, as it yields both high sp^3 carbon content and significant structural disorder. The analysis through Raman spectroscopy indicates substantially lower sp^3-hybridized bond concentrations at 200 V and 250 V discharge voltages. Increasing discharge voltage promotes greater structural disorder, which, along with the decreasing I_D/I_G ratio, confirms enhanced sp^3 bond formation in the coatings.

Figure 3 presents the RMS roughness and grain size D dependencies for ta-C coatings deposited without filtration at various discharge voltages, as measured by AFM.

As a result of the analysis of the dependencies shown in Fig. 3, the following conclusions can be drawn:

a) The RMS roughness of coatings at low voltage (up to 250 V) remains almost unchanged, which is due to its small thickness and possibly island surface morphology.

b) When reaching a voltage of 300 V, a sharp increase is observed with an insignificant change relative to the RMS roughness for ta-C coatings obtained

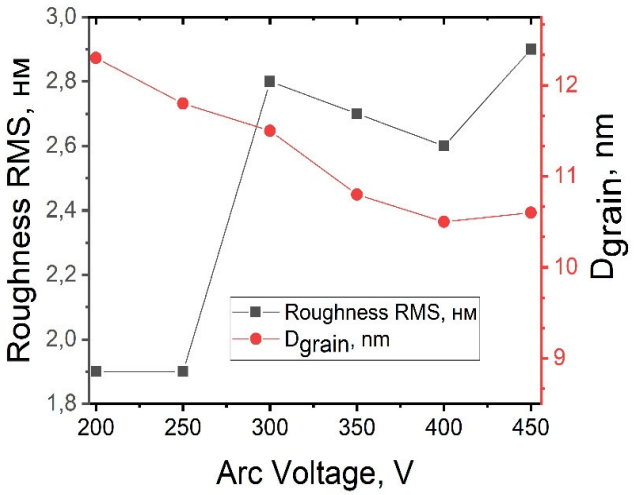

Fig. 3. Roughness RMS and grain size D dependencies for ta-C coatings deposited without flow filtration at various discharge voltages.

at a discharge voltage of more than 300 V. This behavior is possibly associated with the peculiarities of the formation of the coating structure, in particular with an increase in the substrate temperature with an increase in the discharge voltage.

The grain size D exhibits a monotonic decrease with increasing discharge voltage, which, according to previous studies [31], leads to enhanced hardness and density of the resulting coatings.

Thus, the following operating mode of the evaporator is selected.

The deposition of the coatings took place at an initial voltage of the pulsed arc discharge of 300 V, a repetition rate of discharge pulses of 5 Hz and a number of pulses of 1000. Charging the capacitors up to a voltage of 300 V provided the formation of pulse currents up to 5 kA and a discharge duration of 275 μs (the duration depended on the presence of the filter and was determined by its parameters). Carbon coatings were deposited both with the use of an electromagnetic filter produced in the form of a curvilinear solenoid with an angle of rotation of the plasma flow by 90 degrees and without it.

Figure 4 shows the Raman spectra of the deposited carbon coatings. All spectra demonstrate a common peculiar feature: a broad, nearly symmetric Raman scattering peak appears in the 1100–1800 cm^{-1} range, with its center located near 1600 cm^{-1}.

According to the data given in [30], the shape of the obtained spectra corresponds to the Raman spectra for the amorphous carbon coatings with a high content of carbon atoms with sp^3-hybridized bonds. Comparing the spectra, it is possible to notice a slight difference both in the shape of the spectrum envelope and in the intensity. The difference in intensity might be associated with different thicknesses of the coatings, which determines the different powers of the scattered signal. At this position of the peak, the maximum for the ta-C coating is shifted to the region of higher frequencies.

The spectra can be represented by two Gaussian functions centered at 1565 cm^{-1} (peak G) and centered at 1380 cm^{-1} (peak D). The results of mathematical processing of the Raman spectra are shown in Table 1.

Table 1. Results of mathematical processing of the Raman spectra

Sample	G peak position, cm^{-1}	FWHM (G), cm^{-1}	D peak position, cm^{-1}	I_D/I_G
ta-C	1557	204	1383	0.4
ta-C_{filter}	1567	217	1383	0.3

It has been found that for the deposited coatings the intensity ratio of the D and G peaks (I_D/I_G) is slightly different. The I_D/I_G ratio is a measure of the ordering of the sp^2 phase [32], and if it decreases, then the number of ordered aromatic rings in the Csp^2 cluster decreases as well, and the number of chain groups of the C-C type increases [33], which occurs during the deposition of coatings with a plasma flow filtration. At the same time, the G peak position shifts towards higher frequencies, which may indicate an increase in carbon atoms with sp^3-hybridized bonds according to [30]. Consequently, the ta-C_{filter} coating is characterized by an increase in the sp^3-phase compared to the ta-C coating deposited without plasma flow filtration.

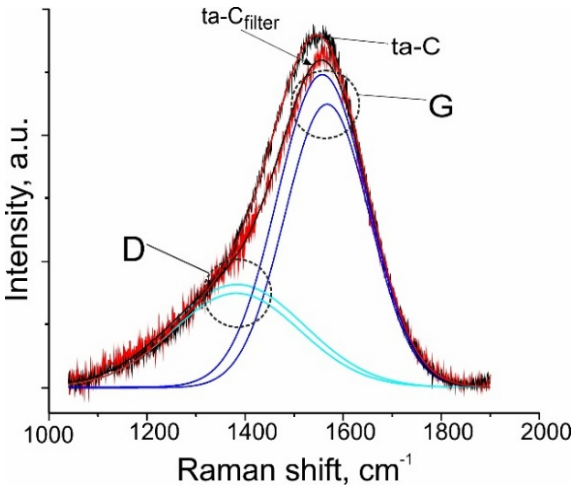

Fig. 4. Raman spectrum for the ta-C coatings deposited from the pulsed discharge plasma and ta-C_{filter} deposited from the filtered pulsed discharge plasma.

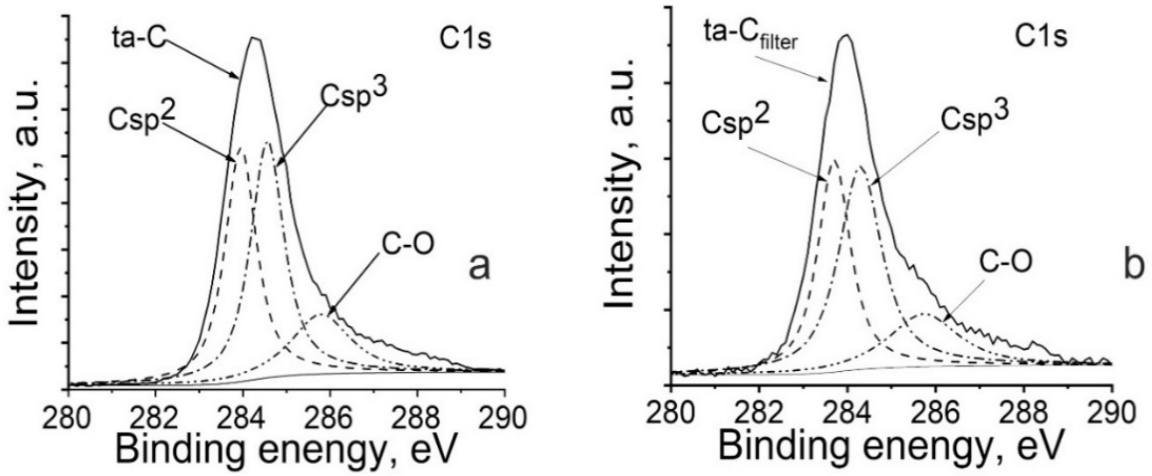

Fig. 5. XPS spectra for the C1s state of carbon atoms in the ta-C coatings deposited from: (a) pulsed discharge plasma, (b) filtered pulsed discharge plasma.

Accordingly, based on the analysis of the Raman spectra parameters for these coatings, it can be concluded that deposition from the filtered flow leads to structural changes, specifically an increase in the number of atoms in the state with sp^3-hybridized atoms, while the size of the Csp^2 cluster also increases [30].

Figure 5 shows the spectrum of the C1s state characteristic of the ta-C coating. The spectrum contains peaks characteristic of Csp^2, Csp^3 and C–O bonds.

Crystalline graphite and diamond, characterized by the sp^2- and sp^3-hybridization of carbon atoms respectively, possess well-defined electronic structures of surrounding carbon atoms. In XPS spectra, their characteristic peaks centered at 284.3 eV and 285.6 eV display narrow, well-defined Gaussian profiles [34]. It is worth noting that XPS spectra of carbon atoms in ta-C coatings, regardless of deposition methods, depend on the overall chemical environment of all surrounding atoms [34] and cannot always be attributed to a single specific bond type that might dominantly influence the chemical shift of the atom in question. In amorphous structures, carbon atoms can form diverse bonding configurations. For instance, single bonds (characteristic of Csp^3 hybridization) may involve one, two, or three neighboring atoms in either Csp^3 or Csp^2 hybridization states, with bond energies that are not always identical. More complex arrangements are also possible, including multiple bonds (particularly double bonds). Carbon atoms in sp^2 hybridization may exhibit one double bond and two single bonds (>C=), two double bonds (=C=), or three "aromatic" bonds. Therefore, the C1s peak may demonstrate significant broadening [35].

As shown in Fig. 5, the C1s peak can be deconvoluted into three spectral components with intensity maxima at binding energies of approximately 284 eV, 285 eV, and 286 eV, corresponding to sp^2–C, sp^3–C and C–O bonds, respectively [34]. Notably, the ratio of partial contributions from sp^3- and sp^2-hybridized bonds to the total C1s peak intensity differs between carbon coatings deposited with and without a filter. When a filter is used, the Csp^2/Csp^3 ratio decreases from 0.92 to 0.78. Additionally, for ta-C_{filter} coatings, a slight shift of the C1s peak towards lower binding energies may occur. These results indicate that the presence of a filter enhances the relative fraction of the sp^3 phase.

The substantially high oxygen concentration in the coating arises from two primary factors:

1) interaction with oxygen present in the residual atmosphere of the vacuum chamber;

2) interaction with oxygen following the depressurization of the vacuum chamber.

In addition to carbon, the coating contains a significant oxygen content (around 8 wt.%), primarily originating from the MPG-6 grade graphite cathode, which itself has an oxygen concentration of 5.4 wt.%.

The results of mathematical processing of the XPS spectra are shown in Table 2.

Analysis of the data presented in Table 2 indicates that the deposition of the coatings from the pulsed discharge plasma under conditions of plasma flow filtration leads to an increase in the Csp^3 component of the coating. In our opinion, this is associated with the formation of a more uniform coating phase structure and, according to AFM and SEM data, with the components in the coating which are usually fragments of the carbon cathode and are characterized by a graphite structure.

Table 2. Results of mathematical processing of the XPS spectra

Sample	G peak position, cm^{-1}	FWHM (G), cm^{-1}	D peak position, cm^{-1}	I_D/I_G
ta-C	1557	204	1383	0.4
ta-C_{filter}	1567	217	1383	0.3

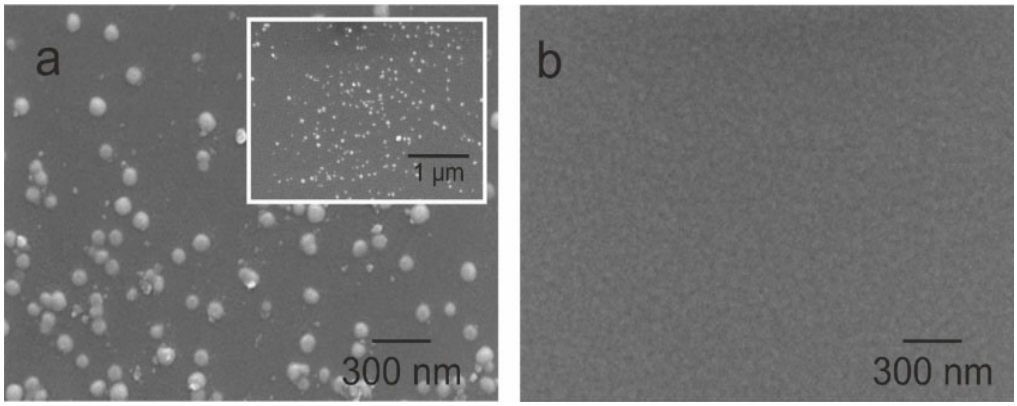

Fig. 6. SEM images of the surface of the ta-C coating deposited from: (a) pulsed discharge plasma, (b) filtered pulsed discharge plasma.

A typical image of the surface of the ta-C and ta-C_{filter} coatings is shown in Fig. 6.

The surface of the ta-C coating has a significant number of particles with a characteristic size ranging from 80 to 100 nm. In this case, for the coating deposition from the flow without filtration (Fig. 6, a), the particle agglomeration (with the size of particles forming a cluster, no more than 200 nm) is observed with an average area up to 3 μm^2.

The additional image (Fig. 6, a) demonstrates the coating surface obtained at a lower magnification and shows that there are a large number of particles on the coating surface. The total area covered by the macroparticles can reach 50% of the substrate area, which leads to a significant decrease in the optical properties of the surface. When using the filter, there is a complete absence of particles on the surface of the substrate. It should be noted that randomly selected areas on the surface of the coating deposited both with and without the filter were compared. What can be stated with a high degree of probability is that the formation of this surface morphology occurs over the entire surface of the substrate. It is shown that the filter removes all large particles, and if there is the formation of charged macroparticles, the transporting magnetic field does not allow them to be kept in the flow because of the low charge/mass ratio, due to which they are removed from the flow. The large length of the filter (380 mm) determines the high efficiency of the flow filtration. However, it significantly reduces the deposition rate and, as the data in Table II show, the ta-C_{filter} thickness is almost 2 times less than the coatings deposited without filtration.

It is also important to note that the ta-C_{filter} coatings do not have particles on the surface. This indicates that a denser flow of the carbon plasma at the exit from the filter leads to an increase in the substrate temperature, which increases the mobility of the deposited particles, suppressing the formation of the structure.

As Fig. 7 shows, the surface morphology of the ta-C coatings differs significantly from the morphology of the ta-C_{filter} coatings. The AFM images display the formation of a smoother surface and a significant decrease in roughness by a factor of 2 in comparison with the coatings deposited from the flows without filtration. The ta-C coating exhibits a surface roughness with an RMS value of 2.8 nm, while the surface has a large number of finely divided globular inclusions with a grain size of 11.5 nm. The coatings deposition from the filtered flow leads to the formation of the coatings with a smaller grain size (D_{grain} = 5.7 nm) and a surface roughness (RMS = 0.5 nm) when compared to flows without filtration. Comparing the phase contrast data (Fig. 7, b and d), it is evident that the application of filtration results in a more uniform phase composition on the surface, with the absence of inclusions that show differing phase compositions. Phase contrast

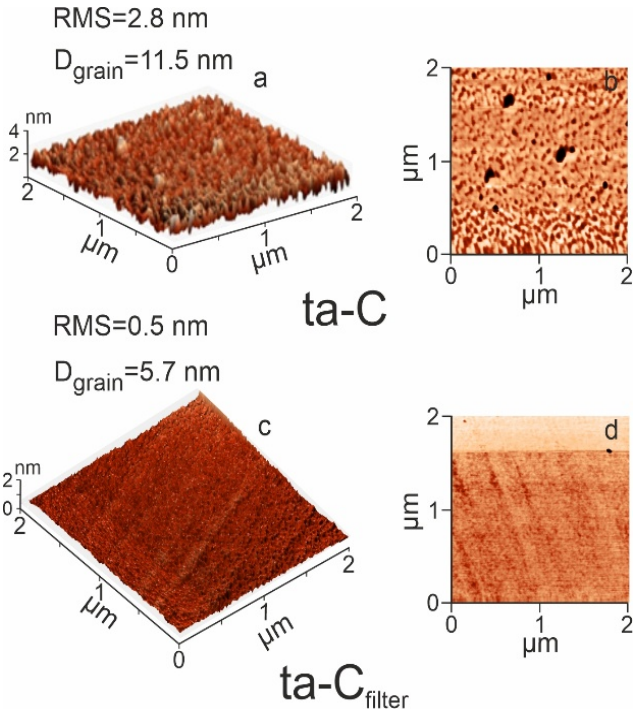

Fig. 7. AFM image of the ta-C and ta-C_{filter} coating: (a, c) topography, (b, d) phase contrast.

images are known to characterize different distributions of mechanical properties over the surface and indirectly indicate different surface distributions of phases.

The analysis of AFM and SEM data reveals that the coatings produced under these deposition conditions are atomically smooth and almost structureless (characterized by an amorphous structure). The nanostructure appears when the coating thickness increases over 300 nm.

The findings regarding the mechanical properties (hardness, elasticity modulus) of the ta-C and ta-C_{filter} coatings are presented in Table 3.

The nanoindentation results for the ta-C_{filter} coating indicate that the application of a filter leads to an increase in nanohardness and Young's modulus, reaching values of 23.4 GPa and 238.1 GPa, respectively, in comparison to the ta-C coating values (Table 3). Despite the decrease in the coating thickness (Table 3), determined by the ellipsometry method, an increase in the sp^3 phase content, confirmed by the XPS method, leads to an increase in the values of mechanical properties.

Table 3. Mechanical properties of the deposited coatings

Sample	d, nm	H, GPa	E, GPa
ta-C	90.8	20.3	208.9
ta-C_{filter}	46.8	23.4	238.1

The results of determining the mechanical properties and optical parameters of the deposited coatings are shown in Table 3 and Fig. 8.

The optical gap E_g is recognized as a key characteristic of non-metallic materials and indicates the type of band structure present in these materials.

The data analysis presented in Fig. 8 demonstrates the change in the refractive index n and the extinction coefficient k of the coatings from the deposition conditions. It has been found that the refractive index changes insignificantly, and the values of the extinction coefficient decrease from 0.031 for the ta-C coating to 0.015 for the ta-C_{filter} coating. The decrease in the extinction coefficient k of the ta-C_{filter} coating is associated with a decrease in the number of Csp^2 clusters, since it is known [36, 37] that the higher the extinction coefficient k, the more graphite-like the coatings are.

The incorporation of inductance in the discharge circuit outside the vacuum chamber (Fig. 1a) during the coating deposition process contributes to a rise in the density of carbon ions, as well as an increase in the number of active particles within the plasma. This phenomenon occurs due to the destruction and secondary ionization of a portion of the droplet component by carbon ions. The secondary carbon ions generated in this case demonstrate a lower energy, which leads to the predominant formation of carbon clusters characterized by sp^2-hybridized bonds, thereby increasing their extinction coefficient. An increase in the refractive index for the ta-C_{filter} coatings is determined by an increase in the concentration of carbon clusters (Table 3, Csp^2/Csp^3 ratio) in the state with sp^3-hybridized bonds, which correlates with the results of determining the hardness and E_g [38].

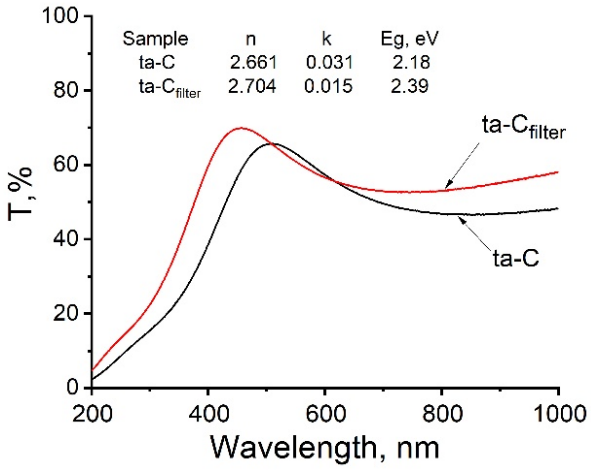

Fig. 8. Transmission spectra in the UV-Vis range and optical parameters for carbon coatings.

The transmittance spectra presented in Fig. 8 demonstrate increased transmittance within the short-wavelength region. This observation aligns with mechanical property measurements and structural-phase analysis, attributed to the enhancement of the sp^3 phase in the coating. The observed increase in E_g values correlates with the alteration of the Csp^2/Csp^3 ratio as well, while the shift of the lower boundary of the absorption band towards the short-wave region of the spectrum suggests a reduction in both the size and quantity of clusters containing Csp^2 bonded carbon atoms [1-3].

4. Conclusions

ta-C coatings have been deposited using a vacuum cathodic-arc discharge technique. The research demonstrates discharge voltage-dependent structural evolution of the coatings and identifies the optimal ta-C deposition mode. The coatings deposited at a discharge voltage of 300 V demonstrate a significant presence of sp^3-hybridized bonds, alongside the maximum RMS surface roughness. A comparative analysis has been conducted on the structure and properties of carbon coatings deposited using the pulsed cathodic-arc method. The implementation of the electromagnetic filter within the anode circuit of the pulsed carbon plasma generator has demonstrated its effectiveness in separating the ionic and droplet components of the coating, while also ensuring the complete removal of macroparticles from the plasma flow. The structural characterization confirms that the use of an electromagnetic filter leads to a decrease in coating roughness, a notable reduction in surface macroparticles, and the formation of a homogeneous phase composition. This leads to a twofold decrease in the RMS surface roughness in comparison with the flow without filtration. The findings indicate a rise in both the hardness and elasticity modulus of the coatings, attributed to an increase in the sp^3 component within the ta-C_{filter} coating.

It has been found that the optical parameters (E_g, n, k) of the coatings depend directly on the phase composition of the coating, which is controlled by the sp^2/sp^3 ratio, and on the parameters of the microstructure (size, number and ordering of sp^2 clusters). The application of filters enables the deposition of coatings composed of amorphous carbon, which exhibit high mechanical and optical properties, and are notably thinner than coatings applied from flows without filtration. The coatings developed can be applied in optics, specifically to protect salt-based optics, as well as to reinforce micro-sized tools designed for drilling circuit boards for soldering microelectronic components. In these applications, high precision is essential, and the presence of macroparticles on the tool's surface can compromise drilling quality.

Acknowledgments

This study was supported by the Intergovernmental Cooperation Projects in the National Key Research and Development Plan of the Ministry of Science and Technology of PRC (No. 2022YFE0196800). The Raman spectrometry was performed on the equipment of CKP "VTAN" in ATRC department of NSU. The research has been carried out within the framework of the NSU program "Strategic Academic Units" (2019) and Ministry of Education of the Republic of Belarus (project 20212075).

References

[1]. Abdul Wasy Zia, Martin Birkett, Deposition of diamond-like carbon coatings: Conventional to non-conventional approaches for emerging markets, *Ceram. Int*. 47 (2021) 28075–28085. DOI: 10.1016/j.ceramint.2021.07.005

[2]. M. Kano, Overview of DLC-Coated Engine Components. In: Cha, S., Erdemir, A. (eds) Coating Technology for Vehicle Applications. Springer, Cham. DOI: 10.1007/978-3-319-14771-0_3

[3]. Bing Zhou, Xiaohong Jiang, A.V. Rogachev, et al., Growth and characteristics of diamond-like carbon films with titanium and titanium nitride functional layers by cathode arc plasma, *Surf. Coat. Technol.* 223 (2013) 17–23. DOI: 10.1016/j.surfcoat.2013.02.020

[4]. K. Bewilogua, D. Hofmann, History of diamond-like carbon films – From first experiments to worldwide applications, *Surf. Coat. Technol.* 242 (2014) 214–225. DOI: 10.1016/j.surfcoat.2014.01.031

[5]. Raj Shah, Nikhil Pai, Rahul Khandekar, et al., DLC coatings in biomedical applications – Review on current advantages, existing challenges, and future directions, *Surf. Coat. Technol.* 487 (2024) 131006. DOI: 10.1016/j.surfcoat.2024.131006

[6]. A.S. Chaus, T.N. Fedosenko, A.V. Rogachev, Ľ. Čaplovič, Surface, microstructure and optical properties of copper-doped diamond-like carbon coating deposited in pulsed cathodic arc plasma, *Diam. Relat. Mater.* 42 (2014) 64–70. DOI: 10.1016/j.diamond.2014.01.001

[7]. V.I. Bogdanovich, M.G. Giorbelidze, Ion-plasma

coatings performance properties improvement obtained by arc deposition, *IOP Conf. Ser.: Mater. Sci. Eng.* 1118 (2021) 012005. DOI: 10.1088/1757-899X/1118/1/012005

[8]. A. Das, B. Chakraborty, A.K. Sood, Raman spectroscopy of graphene on different substrates and influence of defects, *Bull. Mater. Sci.* 31 (2008) 579–584. DOI: 10.1007/s12034-008-0090-5

[9]. A. Anders, Growth and decay of macroparticles: A feasible approach to clean vacuum arc plasmas? *J. Appl. Phys.* 82 (1997) 3679–3688. DOI: 10.1063/1.365731

[10]. S. Chepkasov, M. Khomyakov, A. Zolkin, et al., The Effect of the Substrate Spatial Orientation on The Properties of Amorphous Carbon Coatings Deposited from Pulse Plasma Flows. 2020 7th International Congress on Energy Fluxes and Radiation Effects (EFRE) 7 (2020) 856–862. DOI: 10.1109/EFRE47760.2020.9242030

[11]. B.F. Coll, P. Sathrum, R. Aharonov, M.A. Tamor, Diamond-like carbon films synthesized by cathodic arc evaporation, *Thin Solid Films* 209 (1992) 165–173. DOI: 10.1016/0040-6090(92)90670-7

[12]. P.D. Swift, Macroparticles in films deposited by steered cathodic arc, *J. Phys. D: Appl. Phys.* 29 (1996) 2025. DOI: 10.1088/0022-3727/29/7/041

[13]. S. Boelens, H. Veltrop. Hard coatings of TiN, (TiHf) N and (TiNb)N deposited by random and steered arc evaporation, *Surf. Coat. Technol.* 33 (1987) 63–71. DOI: 10.1016/0257-8972(87)90177-0

[14]. B. Engers, H. Fuchs, J. Schultz, et al. Comparison of substrate temperature and deposition rate between modified pulsed arc process and d.c. arc process. *Surf. Coat. Technol.* 133–134 (2000) 121–125.DOI: 10.1016/S0257-8972(00)00885-9

[15]. E. Hettkamp, H. Mecke, The influence on the plasma and the coating caused through a combination of steered arc and modified pulsed arc processes. *Surf. Coat. Technol.* 200 (2005) 634–638. DOI: 10.1016/j.surfcoat.2005.02.043

[16]. M. Büschel, W. Grimm, Influence of the pulsing of the current of a vacuum arc on rate and droplets, *Surf. Coat. Technol.* 142-144 (2001) 665–668. DOI: 10.1016/S0257-8972(01)01254-3

[17]. H.-S. Zhang, K. Komvopoulos, Direct-current cathodic vacuum arc system with magnetic-field mechanism for plasma stabilization. *Rev. Sci. Instrum.* 79 (2008) 073905. DOI: 10.1063/1.2949128

[18]. Woo-Young Lee, Young-Jun Jang, Takayuki Tokoroyama, et al., Effect of defects on wear behavior in ta-C coating prepared by filtered cathodic vacuum arc deposition, *Diam. Relat. Mater.* 105 (2020) 107789. DOI: 10.1016/j.diamond.2020.107789

[19]. Luyang Ren, Xuhui Liu, Hongshuai Cao, et al., Mechanical and corrosion properties of hydrogen-free DLC coatings prepared on degradable as-extruded WE43 alloy using FCVA technology, *Surf. Coat. Technol.* 476 (2024) 130293. DOI: 10.1016/j.surfcoat.2023.130293

[20]. Hongshuai Cao, Xue Ye, Hao Li, et al., Microstructure, mechanical and tribological properties of multilayer Ti-DLC thick films on Al alloys by filtered cathodic vacuum arc technology, *Mater. Des.* 198 (2021) 109320. DOI: 10.1016/j.matdes.2020.109320

[21]. Ritwik Kumar Roy, Kwang-Ryeol Lee, Biomedical applications of diamond-like carbon coatings: A review, *J. Biomed. Mater. Res. B.* 83 (2007) 72–84. DOI: 10.1002/jbm.b.30768

[22]. A. Stanishevsky, L. Khriachtchev, I. Akula, Deposition of carbon films containing nitrogen by filtered pulsed cathodic arc discharge method, *Diam. Relat. Mater.* 7 (1998) 1190–1195. DOI:10.1016/S0925-9635(98)00174-5

[23]. A.C. Fischer-Cripps, Nanoindentation New York: Springer, 2011. DOI: 10.1007/978-1-4419-9872-9

[24]. Xiaodong Li, Bharat Bhushan, A review of nanoindentation continuous stiffness measurement technique and its applications, *Mater. Charact.* 48 (2002) 11–36. DOI: 10.1016/S1044-5803(02)00192-4

[25]. J. Tauc, R. Grigorovici, A. Vancu, Optical Properties and Electronic Structure of Amorphous Germanium, *Phys. Status Solidi* 15 (1966) 627–637. DOI: 10.1002/pssb.19660150224

[26]. A.V. Stanishevsky, Fabrication, characterization, and postprocessing of cathodic-arc-derived hydrogen-free tetrahedral amorphous carbon. In H.S. Nalwa (ed.), Handbook of Surfaces and Interfaces of Materials, Academic Press 2001, 282–334. DOI: 10.1016/B978-012513910-6/50051-7

[27]. Y. Lifshitz, S.R. Kasi, J.W. Rabalais, W. Eckstein, Subplantation model for film growth from hyperthermal species, *Phys. Rev. B* 41 (1990) 10468. DOI: 10.1103/PhysRevB.41.10468

[28]. J. Robertson, Amorphous carbon, *Adv. Phys.* 35 (1986) 317–374. DOI: 10.1080/00018738600101911

[29]. P Yang, J.Y Chen, Y.X Leng, et al. Effect of annealing on structure and biomedical properties of amorphous hydrogenated carbon films, *Surf. Coat. Technol.* 186 (2004) 125–130. DOI: 10.1016/j.surfcoat.2004.04.039

[30]. A. C. Ferrari, J. Robertson. Interpretation of Raman spectra of disordered and amorphous carbon. *Phys. Rev. B.* 61 (2000) 14095. DOI: 10.1103/PhysRevB.61.14095

[31]. Bing Ye, Xiao Hong Jiang, Bing Zhou, et al., Influences of pulse frequency on structure and mechanical properties of DLC films synthesized by pulsed cathodic arc evaporation, *Appl. Mech. Mater.* 670-671 (2014) 560–564. DOI: 10.4028/www.scientific.net/AMM.670-671.560

[32]. M. Chhowalla, A.C. Ferrari, J. Robertson, G.A.J. Amaratunga, Evolution of sp^2 bonding with deposition temperature in tetrahedral amorphous carbon studied by Raman spectroscopy, *Appl. Phys. Lett.* 76 (2000) 1419–1421. DOI: 10.1063/1.126050

[33]. J. Robertson, Diamond-like amorphous carbon, *Mater. Sci. Eng. R-Rep.* 37 (2002) 129–281. DOI: 10.1016/S0927-796X(02)00005-0

[34]. Yuzhao Zhuang, Xiaohong Jiang, A.V. Rogachev, et. al., Influences of pulse frequency on the structure and anti-corrosion properties of the a-C:Cr films, *Appl. Surf. Sci.* 351 (2015) 1197. DOI: 10.1016/j.apsusc.2015.05.157

[35]. A.T. Kozakov, A.G. Kochur, N. Kumar, et al., Determination of sp^2 and sp^3 phase fractions on the surface of diamond films from C1s, valence band X-ray photoelectron spectra and CKVV X-ray-excited Auger spectra, *Appl. Surf. Sci.* 536 (2021) 147807. DOI: 10.1016/j.apsusc.2020.147807

[36]. E. Pascual, C. Serra, J. Esteve, E. Bertran, Ellipsometric study of diamond-like thin films, *Surf. Coat. Technol.* 47 (1991) 263–268. DOI: 10.1016/0257-8972(91)90290-D

[37]. M. Hiratsuka, H. Nakamori, Y. Kogo, et al. Correlation between optical properties and hardness of diamond-like carbon films, *J. Solid. Mech. Mater. Eng.* 7 (2013) 187–198. DOI: 10.1299/jmmp.7.187

[38]. Jiaqi Zhu, Jiecai Han, Xiao Han, et al., Optical properties of amorphous diamond films evaluated by non-destructive spectroscopic ellipsometry, *Opt. Mater.* 28 (2006) 473–479. DOI: 10.1016/j.optmat.2005.04.008